Journal of Biomolecular NMR, 1 (1991) 299–304
ESCOM

J-Bio NMR 039

Improved three-dimensional ^{1}H-^{13}C-^{1}H correlation spectroscopy of a ^{13}C-labeled protein using constant-time evolution

Mitsuhiko Ikura, Lewis E. Kay and Ad Bax

Laboratory of Chemical Physics, National Institute of Diabetes and Digestive and Kidney Diseases, National Institutes of Health, Bethesda, MD 20892, U.S.A.

Received 18 June 1991
Accepted 2 August 1991

Keywords: 3D NMR; J connectivity; Resonance assignment; Isotopic labeling; Proteins; Calmodulin

SUMMARY

An improved version of the three-dimensional HCCH-COSY NMR experiment is described that correlates the resonances of geminal and vicinal proton pairs with the chemical shift of the ^{13}C nucleus attached to one of the protons. The experiment uses constant-time evolution of transverse ^{13}C magnetization which optimizes transfer of magnetization and thus improves the sensitivity of the experiment over the original scheme. The experiment is demonstrated for calmodulin complexed with a 26-residue peptide comprising the binding site of skeletal muscle myosin light chain kinase.

J correlation of ^{1}H resonances in larger proteins is generally difficult because many of the ^{1}H line widths are larger than the relevant vicinal ^{1}H-^{1}H J couplings. An elegant solution to this problem, which also permits dispersion of the 2D ^{1}H-^{1}H J correlation spectrum into a third dimension (the ^{13}C shift), transfers magnetization in three steps: first from a ^{1}H to its directly attached ^{13}C nucleus via the $^1J_{CH}$ coupling, then from the ^{13}C to its neighbors via the $^1J_{CC}$ couplings, and finally from the ^{13}C nuclei back to their attached protons via $^1J_{CH}$ (Kay et al., 1990; Bax et al., 1990a). For larger proteins this three-step transfer is vastly more efficient than transferring ^{1}H magnetization in a single step using the unresolved ^{1}H-^{1}H J coupling. Transfer of magnetization from one ^{13}C to its neighbors can be accomplished either by a single ^{13}C 90° pulse in a COSY manner, or by isotropic mixing (Braunschweiler and Ernst, 1983; Bax and Davis, 1985) of ^{13}C magnetization (Fesik et al., 1990; Bax et al., 1990b). The corresponding pulse schemes, HCCH-COSY and HCCH-TOCSY, provide complementary information much in the same way as the regular ^{1}H-^{1}H COSY and HOHAHA/TOCSY experiments. Spectral resolution in the HCCH-COSY 3D spectrum is hampered by the fact that the line shape in the ^{13}C dimension is that of a ^{13}C multiplet with the active J_{CC} coupling antiphase and passive ^{13}C-^{13}C couplings in phase. The

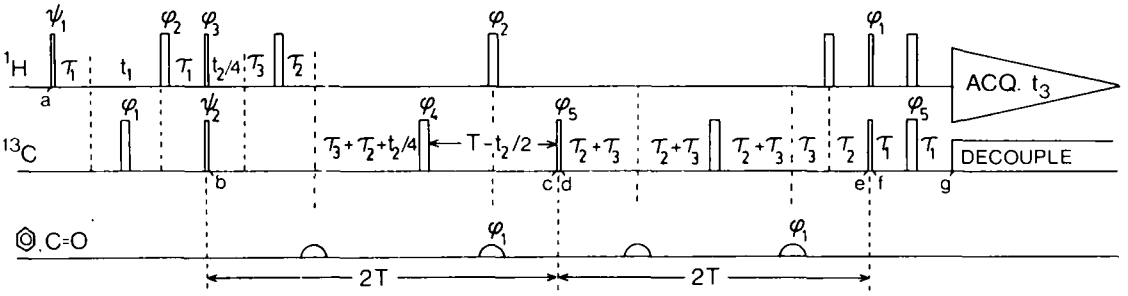

Fig. 1. Pulse scheme of the constant-time HCCH-COSY experiment. All narrow pulses have a flip angle of 90°, the wider pulses have a 180° flip angle. Pulses for which the phase is not indicated are applied along the x axis. The synchronous low power ^{13}C GARP decoupling is preceded by a high power 90_x90_0 pulse pair (not shown) in a manner described previously (Bax et al., 1990a). Phase cycling for θ is: $\theta = 4(x),4(-x)$. Shaped 180° pulses are applied simultaneously to the carbonyl and aromatic Cγ carbons using the center lobe of a sin(x)/x function. The pulses are applied 20.2 kHz (134 ppm) and 13.6 kHz (90 ppm) downfield from the carbon carrier frequency (43 ppm) by using phase modulation of the shaped pulse profile (Boyd and Soffe, 1989). The profile of the shaped pulse is given by $P(t) = (e^{-i\beta_1 t} + e^{-i\beta_2 t})\sin(Ct)/Ct$, where C is set to 20932 and t ranges from −150 to +150 μs (giving a total duration of 300 μs for the center lobe of the sinc function) and $\beta_1 = 20200*2\pi$ and $\beta_2 = 13600*2\pi$ are the angular offset frequencies of the carbonyl and aromatic resonances. The delay durations are: $\tau_1 = 1.6$ ms; $\tau_2 = 1.1$ ms; $\tau_3 = 0.85$ ms. Phase cycling used is as follows: $\varphi_1 = 8(x), 8(-x)$; $\varphi_2 = 4(x),4(y),4(-x),4(-y)$; $\varphi_3 = y,-y$; $\varphi_4 = 2(x),2(y),2(-x),2(-y)$; $\varphi_5 = 4(x),4(-x)$; Acq. = x, −x, −x,x,2(−x,x,x,−x),x,−x,−x,x. The duration of the constant time, T, equals 3.9 ms. Quadrature in the t_1 and t_2 dimensions is obtained using the TPPI-States technique (Marion et al., 1989), incrementing the phases ψ_1 and ψ_2.

antiphase nature of this typically unresolved ^{13}C multiplet causes problems in regions with spectral overlap. Moreover, in the original HCCH-COSY scheme (Kay et al., 1990; Bax et al., 1990a) the efficiency of ^{13}C-^{13}C magnetization transfer depends on the duration of the ^{13}C evolution period, t_2, in a $\sin(\pi J_{CC} t_2)$ manner. Here we describe an improved version of the HCCH-COSY experiment that utilizes constant-time evolution (Bax et al., 1979; Rance et al., 1984) of the ^{13}C magnetization, thus optimizing the ^{13}C-^{13}C magnetization transfer independent of t_2, and removing the multiplet structure in the ^{13}C dimension of the HCCH-COSY spectrum. Analogous improvements for the triple resonance HCACO and HCA(CO)N experiments recently have been reported by Powers et al. (1991).

The pulse scheme of the constant-time HCCH-COSY technique is shown in Fig. 1. Using the product operator formalism (Ernst et al., 1987), the relevant magnetization transfer steps are outlined below. For clarity, relaxation terms are not included and constant multiplicative factors are omitted. Only terms that result in observable magnetization during the detection period, t_3, are retained. The spin operators used are I_1 for the originating and I_2 for the destination proton and S_1 and S_2 for their directly attached ^{13}C nuclei. The effects of multiple bond couplings are neglected throughout and one-bond coupling between spin S_1 and carbon k is denoted by J_{S_1k}; the one-bond coupling between S_1 and its directly attached proton(s) is $J_{S_1I_1}$.

Longitudinal magnetization of proton I_1 and present at time a in the scheme of Fig. 1 is described by a term $\sigma_a = I_{1_z}$. At the end of the evolution time ^1H magnetization is transferred to ^{13}C in an INEPT-type manner. Note that the number of 180° ^{13}C pulses between time points a and b has been reduced to one by concatenation (Kay et al., 1991). At time b, the term of interest is given by:

$$\sigma_b = \cos(\Omega_{1_1} t_1)\sin(2\pi J_{S_1I_1}\tau_1)\, S_{1_y} I_{1_z} \tag{1}$$

During the interval between time points *b* and *c* the effects of one-bond carbon-carbon couplings to backbone or side-chain carbonyls and between Cβ and Cγ resonances of aromatic residues are removed by the selective 180° pulses applied simultaneously to the carbonyl and aromatic spins. It is important that side lobes of these pulses do not affect the aliphatic resonances. However, it is also important that their durations are kept short because, within the limitations of our pulse programmer, they reduce the maximum value of t_2 for a given value of T, i.e., their length reduces the obtainable resolution in the t_2 dimension. It is therefore important to apply the two selective pulses simultaneously. As a compromise for a short 180° pulse without significant side lobes in the aliphatic region of the spectrum we use the center lobe of a sin(x)/x function.

The total time duration between time points *b* and *c* is kept fixed at 2T, which is set to 7.8 ms (vide infra). Two 180° ^{1}H pulses are applied at the times indicated in the pulse scheme to ensure that the ^{13}C magnetization is in-phase with respect to I_1 at time *c*, independent of the duration of t_2. At time *c*, the carbon magnetization of interest is described by:

$$\sigma_c = A\cos(\Omega_{S_1} t_2)\sin(2\pi J_{S_1S_2}T)(\prod_k \cos(2\pi J_{S_1k}T))\, S_{1_z}S_{2_z} \tag{2}$$

where the Π product extends over all carbons *k* coupled to S_1, excluding S_2 and aromatic or carbonyl carbons. Refocusing of antiphase ^{13}C magnetization (present at time *b*) occurs at different rates for methine, methylene and methyl carbons (Burum and Ernst, 1980). For the case where S_1 is a methine carbon, $A = \sin(2\pi J_{I_1S_1}\tau_2)$, for methylenes $A = \sin(4\pi J_{I_1S_1}\tau_2)$, and for methyl groups $A = 0.75(\sin(2\pi J_{I_1S_1}\tau_2) + \sin(6\pi J_{I_1S_1}\tau_2))$. Note that for simplicity the sine and cosine terms of expression (1) have not been carried over to (2). Again omitting the sine and cosine terms from expression (2), one finds at time *d*:

$$\sigma_d = S_{1_z}S_{2_y} \tag{3}$$

During the following time interval of duration 2T, equal to $4\tau_2 + 4\tau_3$, the antiphase S_2 ^{13}C magnetization becomes in phase with respect to S_1 and antiphase with respect to I_2, yielding at time *e*:

$$\sigma_e = B\sin(2\pi J_{S_1S_2}T)(\prod_m \cos(2\pi J_{S_2m}T))\, S_{2_y}I_{2_z} \tag{4}$$

where the Π product now extends over all carbons *m* coupled to S_2, again excluding S_1 and aromatic or carbonyl carbons. For the case where S_2 is a methine carbon $B = \sin(2\pi J_{I_2S_2}\tau_2)$, for methylenes $B = \sin(4\pi J_{I_2S_2}\tau_2)$, and for methyl groups $B = 0.75(\sin(2\pi J_{I_2S_2}\tau_2) + \sin(6\pi J_{I_2S_2}\tau_2))$. At time *f*, the ^{13}C magnetization is converted back into antiphase I_2 spin magnetization:

$$\sigma_f = S_{2_z}I_{2_y} \tag{5}$$

Finally, at the start of the detection period, magnetization is described by:

$$\begin{aligned}\sigma_g = I_{2_y} A*B*\cos(\Omega_{I_1}t_1)\sin(2\pi J_{S_1I_1}\tau_1)\cos(\Omega_{S_1}t_2)\sin^2(2\pi J_{S_1S_2}T)\\ (\prod_k \cos(2\pi J_{S_1k}T))(\prod_m \cos(2\pi J_{S_2m}T))\sin(2\pi J_{S_2I_2}\tau_1)\end{aligned} \tag{6}$$

where the previously omitted sine and cosine terms have been reintroduced. To maximize the magnetization transfer simultaneously for methine, methylene and methyl carbons, a value $\tau_2 \approx 0.3/J_{IS} \approx 1.1$ ms is close to optimal. Alternatively, if one wanted to suppress magnetization transfer to or from methylene or methyl sites, a longer value for τ_2 could be used. This also would result in a modest increase in sensitivity for the selected methine resonances. Minor modifications of the pulse scheme of Fig. 1 also offer the possibility for more extensive spectral editing of the final 3D spectrum. However, for the proteins studied in our laboratory so far this need has not yet arisen.

The acquisition time in the constant-time experiments is limited to $t_2 < 2T$. As can be seen from expression (6), a value for 2T significantly longer than $1/(4J_{CC})$ decreases sensitivity in the presence of passive carbons, particularly when transverse relaxation of the spins S_1 and S_2 is taken into account. In practice, a value of $2T \sim 7.8$ ms is close to optimum and provides sufficient digital resolution in the ^{13}C dimension of the resulting 3D spectrum. Moreover, since the signal does not decay in the t_2 dimension it is ideally suited for linear prediction with mirror image constraint (Zhu and Bax, 1990).

The technique is illustrated for the protein calmodulin, complexed with a 26-residue unlabeled peptide that comprises the binding site of rabbit skeletal muscle myosin light chain kinase. Eight

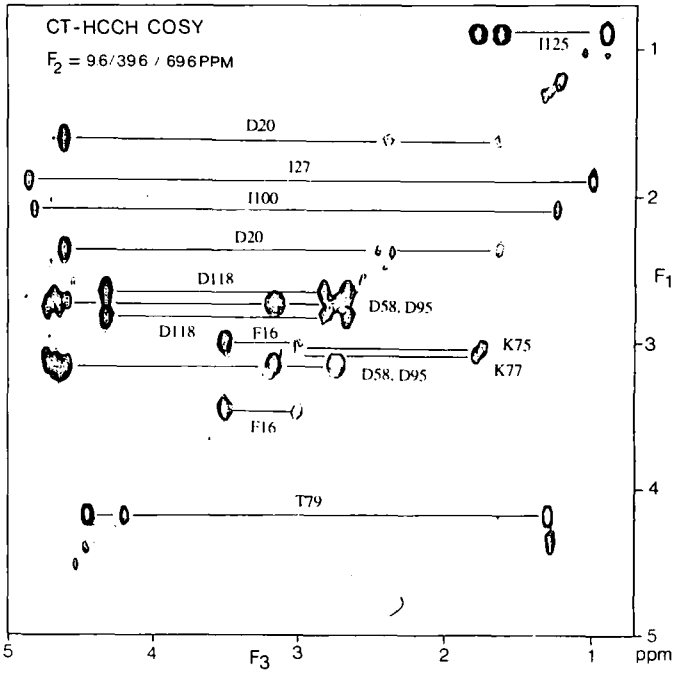

Fig. 2. F_1/F_3 slice of the constant-time HCCH-COSY spectrum of a 1 mM solution of the calmodulin-peptide complex, recorded at 600 MHz, 35°C, p²H 6.8. Resonances on the diagonal ($F_1 = F_3$) correspond to protons attached to carbons that resonate at $9.6 + N \times 30$ ppm ($N = 0,1,2$). Resonances for residues Ile^{27} and Ile^{100} are more intense in the adjacent slices in the F_2 dimension. The spectrum results from a $128 \times 32 \times 256$ data matrix. After t_1 and t_3 Fourier transformation, mirror image linear prediction (Zhu and Bax, 1990) in the t_2 dimension was used to extend the length of the time domain to twice its original length. After zero filling and Fourier transformation, the matrix size of the absorptive part of the final 3D spectrum is $256 \times 128 \times 512$.

mg of calmodulin, labeled uniformly with both ^{15}N and ^{13}C and complexed with both 4 molar equivalents calcium and one equivalent peptide (total mass of the complex ~19.7 kDa) was dissolved in 0.4 ml D_2O, p^2H 6.8. Experiments were conducted at 35°C on an unmodified Bruker AMX-600 spectrometer. The size of the acquired data matrix was $128 \times 32 \times 256$, where all numbers correspond to complex data points, and the acquisition times were 32 ms (t_1), 7.04 ms (t_2) and 53 ms (t_3). The 16-step phase cycle was executed four times (with different ψ_1 and ψ_2 values) to obtain quadrature in both the t_1 and t_2 dimensions. The delay time between scans was 0.9 s, and the total measuring time was 72 h.

Figure 2 illustrates the quality of the data obtained with the constant-time HCCH-COSY technique. Figure 2 shows a ^1H-^1H slice, taken at a ^{13}C (F_2) shift of 9.6, 39.6 or 69.6 ppm. Note that because the ^{13}C spectral window was only 30 ppm, extensive folding has taken place in this dimension. The resonance in the top right corner of the spectrum corresponds to the Cδ methyl of Ile^{125} and shows intense cross peaks with both non-equivalent Cγ methylene protons. The lowest trace marked in the spectrum shows cross peaks between Thr^{79} Hβ (diagonal) and the Hα and Hγ protons. For J connectivity involving non-equivalent methylene protons, the cross peak intensity is halved relative to interactions involving methyl or methine sites. In addition, since the non-equivalent methylene protons typically have rather large line widths, caused by their large unresolved geminal J_{HH} coupling and their strong geminal dipolar ^1H-^1H interaction, these resonances are attenuated even further. Nevertheless, the sum of the integrated intensities of all cross peaks is invariably larger than the intensity of the corresponding diagonal resonance in the constant-time HCCH-COSY spectrum. At first sight, it appears that the connectivities for Phe^{16} (Fig.

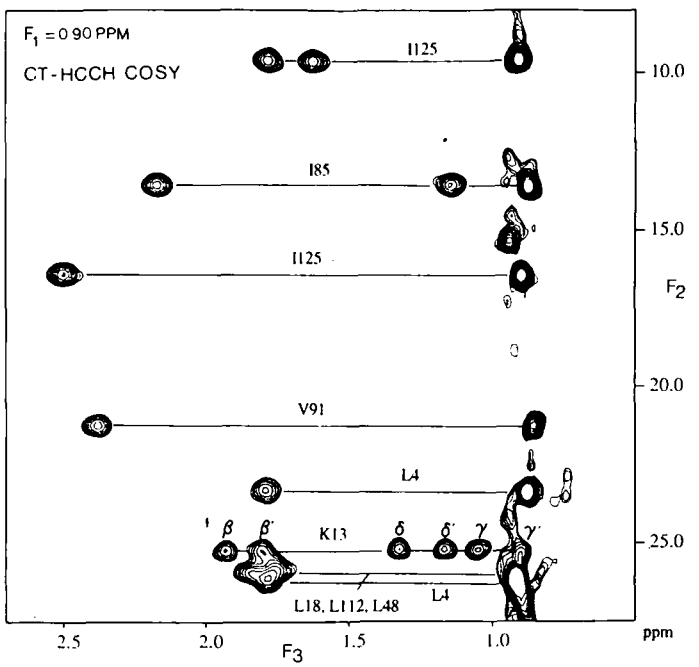

Fig. 3. Section of an F_2/F_3 slice of the constant-time HCCH-COSY spectrum, taken at an F_1 frequency of 0.90 ppm. Resonances near $F_3 = 0.9$ ppm correspond to diagonal resonances in the F_1/F_3 planes.

2) may be exceptions to this rule. However, the pattern for Phe^{16} is unusual since its Hα overlaps with the downfield Hβ resonance and the relatively intense diagonal resonance coincides with the Hα/Hβ cross peak.

Figure 3 shows part of an F_2/F_3 cross section of the 3D spectrum, taken at the F_1 frequency (0.9 ppm) of Ile^{125} $C\delta H_3$. Resonances near $F_3 = 0.9$ ppm correspond to diagonal resonances in the various F_1/F_3 planes and show cross peaks to their vicinal neighbors. With the exception of Lys^{13}, all 'diagonal' resonances in this spectrum correspond to methyl groups. The Lys^{13} 'diagonal' resonance corresponds to one of the two non-equivalent Cγ protons and exhibits cross peaks with its geminal partner and with the non-equivalent Cβ and Cδ protons. The line shape in the F_2 dimension of the spectrum is now an in-phase singlet, whereas it was an antiphase doublet in the original HCCH-COSY experiment (Bax et al., 1990b). We find the in-phase singlet line shape in the present spectrum strongly preferable in regions with substantial overlap compared to the antiphase doublet shape. The improved sensitivity of the constant-time version and the reduced intensity of diagonal resonances are other noteworthy benefits.

ACKNOWLEDGEMENTS

We thank Marius Clore, Stefan Gzresiek, Robert Powers and Dennis Torchia for stimulating discussions during the course of this work, and Guang Zhu for improving the stability of the linear prediction software. This work was supported by the AIDS Targeted Anti-Viral Program of the Office of the Director of the National Institutes of Health.

REFERENCES

Bax, A., Mehlkopf, A.F. and Smidt, J. (1979) *J. Magn. Reson.*, **35**, 167-169.
Bax, A. and Davis, D.G. (1985) *J. Magn. Reson.*, **65**, 355-360.
Bax, A., Clore, G.M., Driscoll, P.C., Gronenborn, A.M., Ikura, M. and Kay, L.E. (1990a) *J. Magn. Reson.*, **87**, 620-627.
Bax, A., Clore, G.M. and Gronenborn, A.M. (1990b) *J. Magn. Reson.*, **88**, 425-431.
Boyd, J. and Soffe, N. (1989) *J. Magn. Reson.*, **85**, 406-413.
Braunschweiler, L. and Ernst, R.R. (1983) *J. Magn. Reson.*, **53**, 521-528.
Burum, D.P. and Ernst, R.R. (1980) *J. Magn. Reson.*, **39**, 163-168.
Ernst, R.R., Bodenhausen, G. and Wokaun, A. (1987) *Principles of Nuclear Magnetic Resonance in One and Two Dimensions*, Clarendon Press, Oxford, pp. 25-32.
Fesik, S.W., Eaton, H.L., Olejniczak, E.T., Zuiderweg, E.R.P., McIntosh, L.P. and Dahlquist, F.W. (1990) *J. Am. Chem. Soc.*, **112**, 886-888.
Kay, L.E., Ikura, M. and Bax, A. (1990) *J. Am. Chem. Soc.*, **112**, 888-889.
Kay, L.E., Ikura, M. and Bax, A. (1991) *J. Magn. Reson.*, **91**, 84-92.
Marion, D., Ikura, M., Tschudin, R. and Bax, A. (1989) *J. Magn. Reson.*, **85**, 393-399.
Powers, R., Gronenborn, A.M., Clore, G.M. and Bax, A. (1991) *J. Magn. Reson.*, in press.
Rance, M., Wagner, G., Sorensen, O.W., Wüthrich, K. and Ernst, R.R. (1984) *J. Magn. Reson.*, **59**, 250-261.
Zhu, G. and Bax, A. (1990) *J. Magn. Reson.*, **90**, 405-410.